Adhesive Joints on Glass fiber Vinylester Lamina

Author: Babish Maden Limbu

Instructor: Rene Herrmann

Degree Thesis

Materials Processing Technology

2018

DEGREE THESIS	
Arcada	
Degree Programme:	Materials Processing Technology
Identification number:	
Author:	Babish Maden Limbu
Title:	Adhesive joints on glass fiber vinyl ester lamina
Supervisor (Arcada):	Rene Hermann
Commissioned by:	

Abstract:

Thesis motive is to experimentally analyse adhesive joint strength and adhesive bonding on glass fiber vinyl ester laminate through 3 point bending test and peel test. Study also shows adhesive joint strength as a function of scarf angle, adhesives, adhesives mixed with additives, initial surface treatment and peel strength.
Procedure is structured by ISO and ASTM's surface preperation, 3 point bending and peel test standards.
Glass fiber vinyl ester laminate is sanded on sanding machine with 120 gird sandpaper on various angles and bonded with WS 105 Epoxy, polyester, vinyl ester, loctite 435 with cellulose, silica and 3 other additives as adhesive. Cured samples are re-sanded to its initial shape. Maximum force data and peel strength data is collected and analyzed.
Scarf joint theory as a function of angle is proven to be true by this study. From stress data, it is observed that WS 105 Epoxy is stronger adhesive bonding resin than polyester, vinyl ester and loctite 435. Cellulose and silica additive increases bonding strength and viscosity while phenol microballs, microballs SG and glass fiber paste only increased viscosity. Adhesive joint strength at 86° degree scarf angle with cellulose and silica additive mixed with Epoxy was able to create cohesive failure of adherent achieving 30,87% of laminate's original strength. Tapered end on scarf joint edge is necessary to prevent peeling stress thus proving Volkersen and Klein theory of adhesive joint strength due to bondline thickness on adhesive joints. Cellulose additive increases peel resistance.

Keywords:	Adhesive, additive, adhesive bonding, scarf angle, scarf joint, stress, 3 point bending, peel test, UD laminate, laminate's original strength
Number of pages:	54
Language:	English
Date of acceptance:	

Contents

Figures

Table

Abbreviation

1. UD lamina – Unidirectional vacuum Laminated Glass fiber Specimen of 6 ply and 8 ply with 1200 g/m^2 in each ply.
2. FPR – Fiber reinforced plastic
3. F_N – Force acting perpendicular to x-axis
4. F_X – Force acting along x-axis
5. σ_N – X-axis perpendicular stress
6. σ_x – X-axis parallel stress
7. τ – Shear stress
8. p – Ratio of strap thickness to laminate thickness
9. e – Strap thickness
10. t – laminate thickness
11. α – Scarf angle
12. A – Cross-section area
13. τ_{Kmax} - Shear stress peak
14. F - Force acting along joint
15. b - Joint breadth
16. E - Young's Modulus of laminate
17. G_k - Laminate Elastic Modulus
18. t_k - Joint thickness
19. M - Bending moment
20. w - Deflection
21. w_0 - Central displacement
22. E - Young's modulus
23. I – 2^{nd} moment of area

FOREWORD

I would like to thank Mr. Rene Herrmann for excellent supervision and guidance thoughout this thesis.

I would also like to thank Mr. Erland Nyorth for his excellent co-ordination in lab during tests. I am also greatful to all the professors and staff for their guidance throughout my studies at Arcada University of Applied Sciences.

Finally, I would like to thank my family and friends for their continued support during my study period. Special thanks to my parents, Dhir Maya Maden and Chhatra Bahadur Maden for support and encouragement to complete this thesis.

1 INTRODUCTION

The **purpose** of this thesis is to study strength of adhesive bond prepared on glass fiber composite laminate using varying bonding agents and additives, joint geometry and surface preparation methods. This study is also dedicated to determine strength of composite specimen by 3 point bending test or peel test.

The **motivation** for this study is to maximize adhesive joint strength. Study is focused in either the maintenance procedure of composite structures or their initial joining.

The main **objective** of the thesis is to find maximum scarf angle that guarantees cohesive failure in the adherent implying that the adhesive bond is stronger than the adherent. To show adhesive bonding is an alternative to bolting/ mechanical fastening is priority of this thesis.

High performance composites are being increasingly used in structures requiring high specific strength and stiffness. Automotive, marine, military, aeronautical and aerospace industries are the main fields of application of these materials. These high responsibility and severely loaded applications introduces an issue regarding the handling of these materials after damage. Repair of these structures should be evaluated, instead of their disposal, for cost saving and ecological purposes.

Fastened repairs present some disadvantages, such as the weight penalty and significant stress concentration at localized regions of the composite structure, which can cause local overloads and premature damage initiation.

In recent years, the use of adhesives in structural applications is growing, achieving a great current implementation in the industry, due to the benefits that this technology is capable of providing to complex-shaped structures, both in aerospace and automotive applications. Adhesive joints show many advantages in comparison with other traditional joints such as welded joints, because they offer a continuous joint with homogeneous stress distribution, they are able to joint dissimilar materials (such metals and composite materials) and they do not require large investments. [1]

1.1 Adhesives

An adhesive is a material applied to surfaces of articles to permanently join them by a bonding process. It is a substance capable of forming bonds to each of the two or more part interfaces comprising the final object and the process is referred as “adhesion”.

Adhesion refers to the state in which two similar or dissimilar bodies are held together by intimate interfacial contact such that mechanical force or work can be transferred across the interface. The interfacial forces holding the two phases together may arise from Van Der Waals forces, chemical bonding, or electrostatic attraction. The mechanical strength of the system is determined not only by the interfacial forces, but also by the mechanical properties of the interfacial zone and the two bulk phases. [2]

Figure 1: Araldite industrial adhesive [3]

There are a large number of adhesive types for various applications. They may be classified in a variety of ways depending on their chemistries (e.g. epoxies, polyurethanes, polyimides), their form (e.g. paste, liquid, film, pellets, tape), their type (e.g. hot melt, reactive hot melt, thermosetting, pressure sensitive, contact, etc.), or their load carrying capability (structural, semi-structural, or non-structural). [4].

Figure 2 is an example of technical datasheet available for commercial adhesive.

Araldite®
Strength in bonding 2000+

Properties and performance

	Chemical type	Key features	Thermosets / composites				Cure speed	Mechanical properties		Bond strength	Durability in			Colour (mixed)
			GRP (UP)	GRP (EP)	CFRP	SMC								
Conditions							Cure time at 23°C to LSS* = 1 N/mm²	E-modulus at 23°C	Elongation at break at 23°C	LSS* aluminium at 23°C	Water / humidity	Chemicals	Heat	
Unit							min	N/mm²	%	N/mm²				
Araldite® 2011	EP	> Multi purpose > Long working life > Good resistance to dynamic loading	•••	•••	•••	•••	420	1900	9	26	•	••	••	yellow
Araldite® 2012	EP	> Fast curing > General purpose > Good long term durability	•••	•••	••	••	20	2520	4	18	••	•••	••	yellow
Araldite® 2013	EP	> Metal coloured paste > Suitable for vertical applications > Good environmental, chemical and temperature durability	•••	••	••	•••	240	1300	1	18	••	••	••	grey
Araldite® 2014-1	EP	> Grey paste > High temperature and chemical resistance > Excellent durability on metals and against many chemicals	•••	•••	••	•••	180	4000	1	19	•••	•••	•••	grey
Araldite® 2015	EP	> Toughened paste > Ideal for GRP, SMC and dissimilar substrates > Excellent resistance to dynamic loading	•••	•••	•••	•••	240	2000	4	16	•••	•••	•••	beige
Araldite® 2031	EP	> Toughened adhesive, resilient bond > Suitable for metal and composite bonding, good adhesion onto polyamides	•••	•••	••	•••	360	1000	5	19	•••	•••	•••	black
Araldite® 2018	PUR	> Good UV stability > Ideal for bonding thermoplastics > Long working life	•••	•••	•••	•••	240	16	45	7	••	•	••	colourless
Araldite® 2028-1	PUR	> Transparent > Fast curing > UV stable	•••	•••	•••	•••	15	16	60	15	•	•	••	transparent
Araldite® 2029	PUR	> Medium open time > Designed to bond composites and metals > Well balanced strength and durability	•••	•••	•••	••	240	580	39	25	••	••	•••	grey
Araldite® 2021	MMA	> Rapid curing > High peel and shear strength > Multi purpose	•••	••	••	••	8	2300	5	23	••	••	•••	yellow
Araldite® 2022	MMA	> Ideal for bonding thermoplastics > Multi purpose > Good sanding properties	•••	••	••	••	18	2050	3	25	••	•	•••	yellow
Araldite® 2047-1	MMA	> Outstanding adhesion to copper, brass, galvanized and stainless steel > Requires minimal surface treatment > Gap filling up to 5 mm	••	•	•	••	15	850	15	19	••	••	••	brown
Araldite® 2048	MMA	> Tolerant to "less than ideal" pretreatment > Gap filling up to 8 mm > Tough flexible bonds for use in dynamic environmen	••	•••	•••	•••	15	360	91	24	••	•	•••	red
Araldite® 2052-1	MMA	> Very high temperature and chemical resistance > Tolerant to "less than ideal" pretreatment > Excellent on metals	•	•	•	•	20	1750	7	24	••	•••	•••	red

EP: Epoxy adhesives
PUR: Polyurethane adhesives
MMA: Methacrylate adhesives

Figure 2: Araldite adhesive technical datasheet. [5]

1.2 Adhesive bonding

Adhesive bonding is used to fasten two surfaces together, usually producing a smooth bond. This joining technique involves glues, epoxies, or various plastic agents that bond by evaporation of a solvent or by curing a bonding agent with heat, pressure, or time. Historically, glues have produced relatively weak bonds. However, the recent use of plastic-based agents such as the new “super-glues” that self-cure with heat has allowed adhesion with a strength approaching that of the bonded materials themselves. As a result, gluing has replaced other joining methods in many applications especially where the bond is not exposed to prolonged heat or weathering. A large fraction of modern glues are carbon-based petrochemical derivatives. These can be used to bond almost any combination of surfaces, either by direct contact or by fastening both surfaces to a third as with adhesive tapes. Glues can serve as bonding agents in strong structural materials. One of the earliest, and still common use is the fabrication of plywood. Other related composites include fiberglass and various fiber-epoxies such as boron-epoxy and carbon-epoxy. [6]

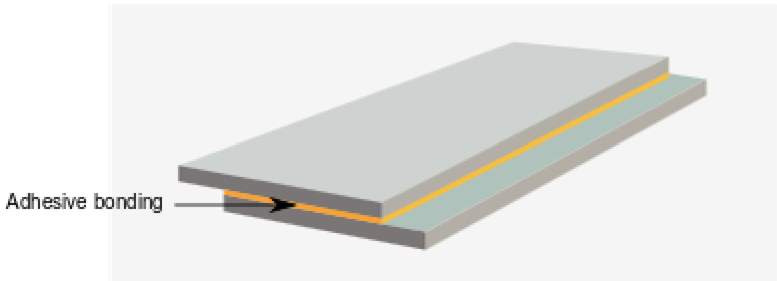

Figure 3: Single lap joint [7]

Limitation for adhesive bonding to mechanical fastening lies on its difficult nature on removal or disassembly process as bond can destroy or distort adherent joint together.

1.3 Adhesive joints stress distribution

Stress acting along adhesive joints due to tension, compression, shear, cleavage and peel loading differ from each other. Cleavage and peel loading concentrates applied force into single line of high stress happens to be most severe loading. Hence, practically it is always wiser to avoid cleavage and peel stresses.

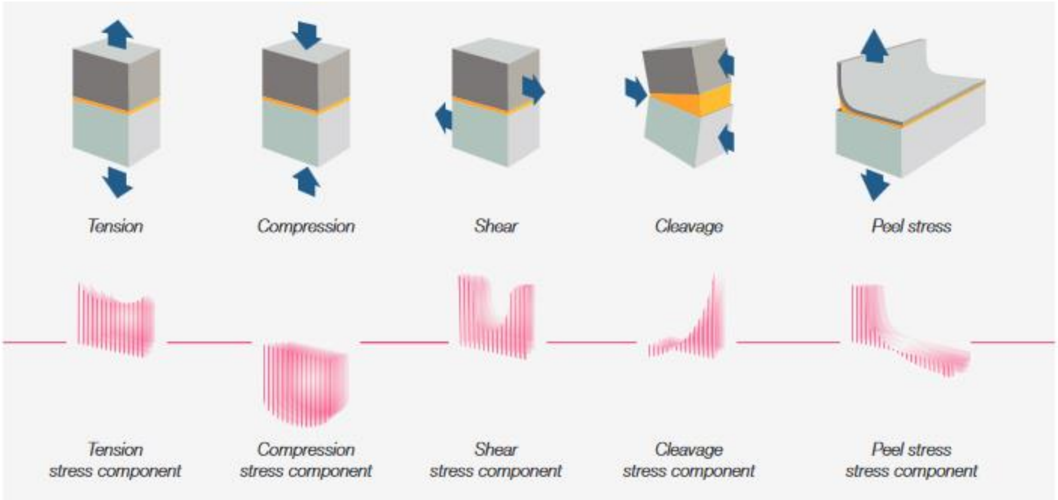

Figure 4: Stress distribution in adhesive joints. [7]

Figure 4, shows stress distribution in adhesive joint due tension, compression, shear, cleavage and peel stress.

1.4 Adhesive joint types

Numerous types of bonded joints exist, overlap, scarf and stepped lap, each of which can be constructed in single or double shear arrangements. In composite structures when high strength recovery is needed, or when there is a requirement for a flush surface to satisfy aerodynamic or stealth requirements, a bonded scarf or stepped repair is used. However, designing an optimum scarf repair for composite structures is complex due to the large number of material and geometric parameters that influence the joint performance. [8]

Furthermore, access limitations or structural design (e.g. sandwich configurations) often limit repairs to single-scarf designs, instead of superior double-scarf or double-stepped lap repairs.

Figure 5 shows summary of various models of adhesive joints. Scarf joint adhesive joint study is the main objective. Bevel joint are scarf joint with step and are used in aircraft structure repairs.

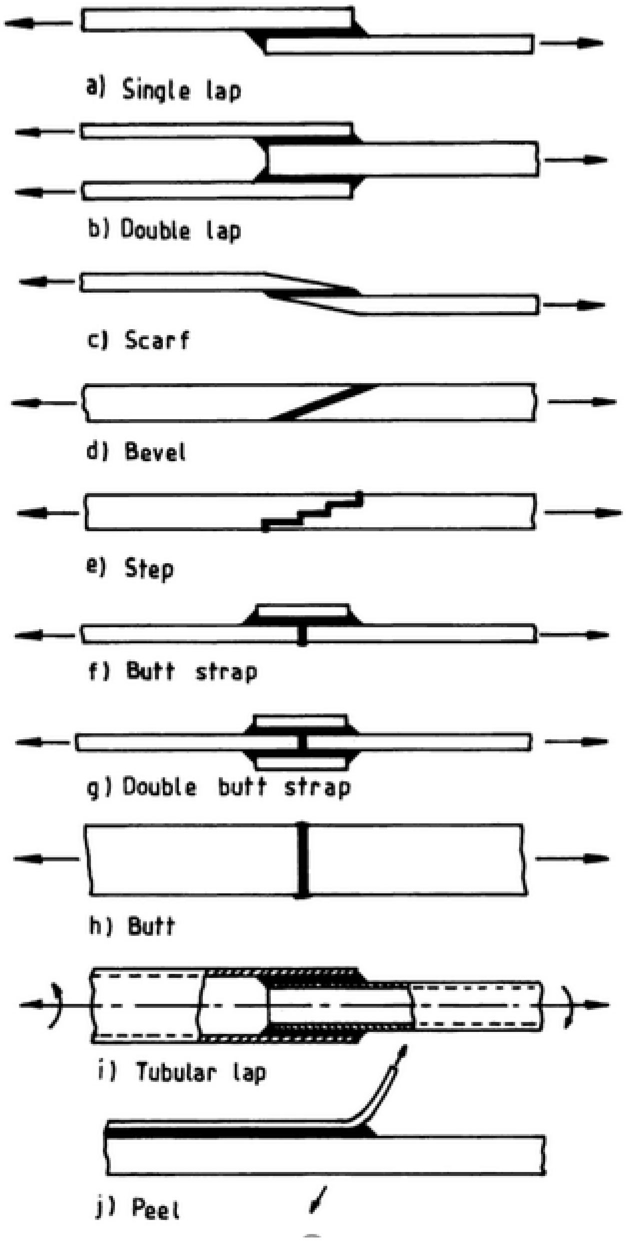

Figure 5: Different kind of adhesive joints. [6]

1.5 Overview of Adhesive and Cohesive bonding

Cohesion is defined as the internal strength of an adhesive as a result of a variety of interactions within the adhesive. Adhesion is the bonding of one material to another, namely an adhesive to a substrate, due to a variety of possible interactions. Figure 6, illustrates adhesion and cohesion forces present within an adhesive and between an adhesive and substrate.

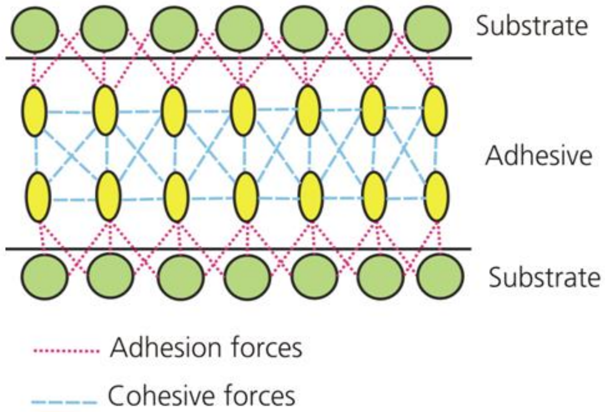

Figure 6: Adhesive and Cohesive force distribution. [9]

Adhesive joint failure types are,

I. ***Cohesive failure*** is described as a failure mode when adherent breaks. It occurs when adhesive joint is stronger than material itself.

II. ***Adhesive failure*** is the failure mode when glue/adhesive breaks. It occurs when adhesive bonding and material is stronger than adhesive.

III. ***Co-adhesive failure*** is the failure mode when interface breaks. It occurs when adhesive bonding isn't proper due to improper priming of joining interface or when adhesive or material is stronger than adhesive bonding.

2 LITERATURE REVIEW

This chapter summarizes the standards existing for loading mechanism of adhesive joint, adhesive joint preparation, design, and adhesive joint testing.

2.1 Standards on loading mechanism of adhesive joints

Adhesive joints loading mechanism varies according to force acting along joints. There are various test methods for determining different kind of adhesive joint properties. Due to similarities in testing method and the type of force acting along adhesive joint, loading mechanism of adhesive joints can be differentiated as tensile/compression loading and cleavage/peel loading.

2.1.1 Tensile loading / Compression loading

Standards provided for tensile and compression loading for glass fiber vinyl ester laminate are,

I. **D3163 - 01(2014) -** Standard test method for determining strength of adhesively bonded rigid plastic lap-Shear joints in Shear by Tensile loading. [10]

II. **D3165 - 07(2014)** – Standard test method for Strength properties of Adhesives in Shear by Tensile loading of Single Lap Joint Laminated assemblies. [10]

III. **D3528 - 96(2016)** – Standard test method for Strength properties of Double Lap Shear Adhesive joints by Tensile loading. [10]

IV. **D905 - 08(2013)** – Standard test method for Strength properties of Adhesive bonds in Shear by Compression loading. [10]

2.1.2 Cleavage / Peel loading

International standards provided for Cleavage / Peel loading for GRP laminate are,

I. **D3807 - 98(2012)** – Standard test method for Strength properties of Adhesives in Cleavage/Peel by Tensile loading.

II. **D1876 - 08(2015) e1** – Standard test method for Peel resistance of Adhesive (T-Peel test).

III. **ISO 15107:1998** – Determination of cleavage strength of bonded joints. [11]

IV. **ISO 11339:2010** – T-peel test for flexible-to-flexible bonded assemblies. [11]

2.2 Standards on joint preparation

Glass fiber vinyl ester laminate joint preparation is done according to following standards,

I. **ISO 17212:2012** provides guidelines for the surface preparation of plastics prior to adhesive bonding. [11]

II. **D2093 - 03(2017)** is Standard practice for preparation of surfaces of plastics prior to Adhesive bonding. [12]

2.3 Standards on joint testing

Determining shear strength by 3 point bending test has been performed according to international standards available for adhesives. Some of the standards are listed below,

I. **ISO 4587:2003 (en)** is the standard used to determine tensile lap-shear strength of rigid-to-rigid bonded assemblies. [11]

II. **ISO 15108:1998** is Standard for determining strength of bonded joints using a bending shear method for Adhesive joints. [11]

III. **D5868 - 01(2014)** is Adhesive standard test method for lap shear adhesion for fiber reinforced plastic (FPR) bonding. [12]

IV. **D3165 - 07(2014)** is Standard test method for strength properties of Adhesives in shear by tension loading single-lap-joint laminated assemblies. [12]

V. **D3528 - 96(2016** is standard test method for strength properties of double lap shear adhesive joints by Tension loading. [12]

2.4 Adhesive certification

Standards Catalogue **83.180 – Adhesives** provided by International Organization for Standardization (ISO) provides all the standards required for adhesive certification.

ASTM International's Adhesive Standards also provides standard required for adhesive certification.

3 MODELS ON JOINT STRESS

This chapter describes theories for stress acting along adhesive bond line for butt joint, butt joint with strap, scarf joint, step scarf joint, Volkersen theory and Klein theory.

3.1 Butt joint theory

Forces acting on joints can be dissected as,

On vertically attached area

- $F_N = F_X$
- $F_T = 0$

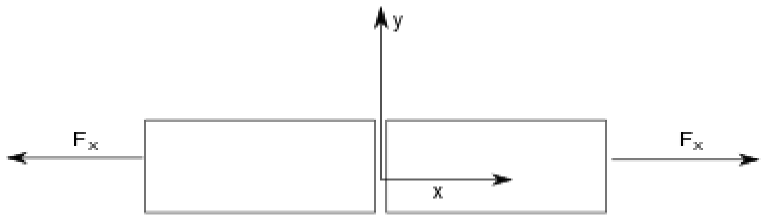

Figure 7: Force acting along Butt joint

Normal stress (σ_N) and shear stress (σ_x) are equal.

$$\sigma_N = \sigma_x = F/A$$

3.2 Butt joint with strap theory

Forces acting on joints can be dissected as,

On vertically attached area

- $F_N = F_X, \sigma_N = \sigma_X$
- $F_T = 0$

On horizontal support area, the strap

- $\sigma_N = \sigma_X \frac{t}{e}$
- $\tau_T = \frac{F_x}{wL_2}$

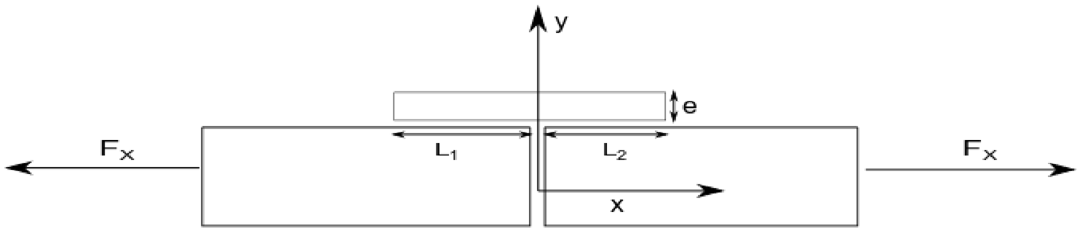

Figure 8: Force acting along butt joint with strap

Here,

I. Total cross-section area in between right angled joints = A
II. Total cross-section area under parallel support = A_1
III. $p = \frac{e}{t}$, ratio between thickness of strap to laminate thickness.

3.2.1 Normal Stress

Normal stress (σ_N) can be derived as:

$$\sigma_N = \frac{\sigma_x}{(1+p)}$$

3.2.2 Shear stress

Shear stress (τ) can be derived as:

$$\tau = \frac{2\sigma_x}{p}$$

3.3 Scarf joint

Scarf repairs are currently the preferred method for repairing thick composite structures to restore the load-carrying capability to its as-designed level. Current design methodology recommends that a scarf repair should match, ply-by-ply, the original structure. With matched adherents, the adhesive stresses along the scarf are assumed to be uniform and the joint is assumed to attain its maximum strength when the average shear stress reaches the ultimate shear strength of the adhesive. [13]

3.3.1 Scarf joint theory

Stress analysis is done under following assumptions and conditions

I. The plane to be 2 dimensional where thickness (t) of the materials is regardless i.e. t=0
II. If angle of contact $\alpha = 90°$, then shear stress on the joint is "0".

3.3.1.1 Forces Dissection

Forces acting on scarf joints can be described as,

$$F_N = F_X \cdot cos\alpha$$

$$F_T = F_X \cdot sin\alpha$$

3.3.1.2 Section

Cross-section area (A) is the function of stress on angle of contact (α)

$$A_\alpha = b\frac{t}{cos\alpha} = \frac{A}{cos\alpha}$$

*I. **Normal Stress***

Normal stress (σ) acting along adhesive is given by:

$$\sigma_\alpha = \sigma_X \cdot \cos^2 \alpha$$

*II. **Shear stress***

Shear stress (τ_α) acting along adhesive is given by:

$$\tau_\alpha = \frac{1}{2}\sigma_X \cdot sin2\alpha$$

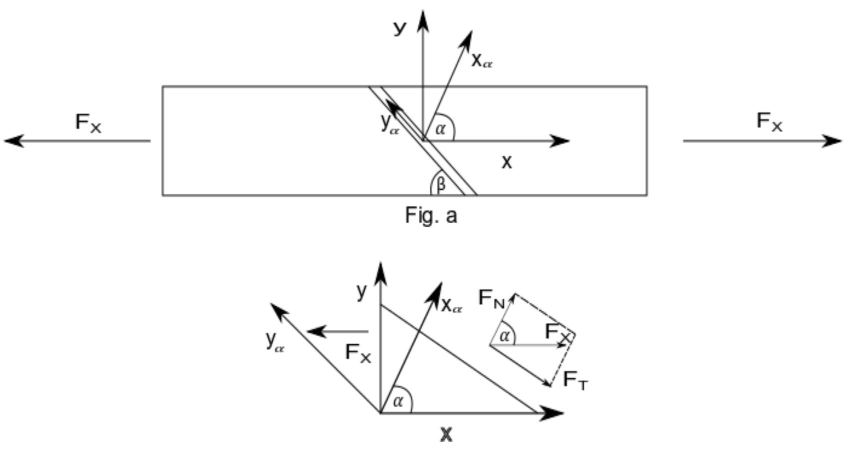

Figure 9: Scarf joint force dissection

Scarf joint theory gives two solution for scarf angle to create optimum adhesive joint strength as shown in figure 10 below,

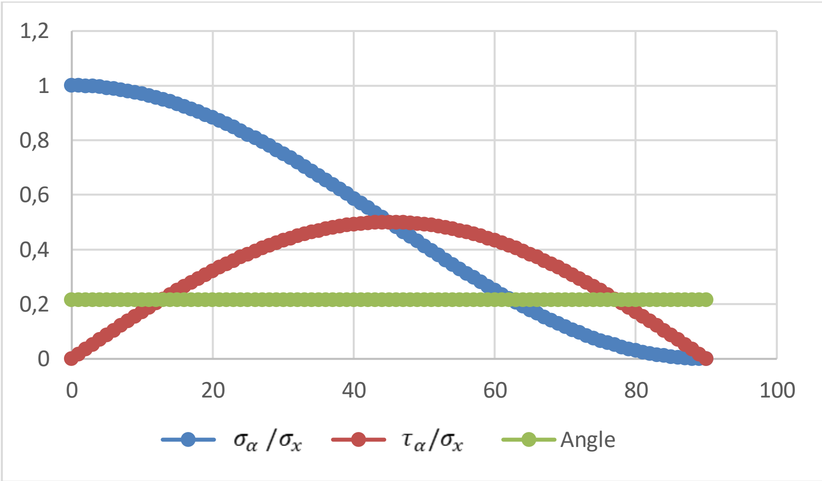

Figure 10: Scarf joint tensile and shear to normal stress ratio

Figure 10, illustrates tensile to normal stress ratio, shear to normal stress ratio and an angle line showing two solutions for maximum strength at scarf joint angle indicated by two intersections on shear stress curve.

Hence, for known technical properties of adherent in adhesive joints, an angle for maximum performance under shear loading can be found by selecting larger angle from graph.

3.4 Scarf joint with step theory

This is a scarf angle and additionally at the mid surface a step. The joint geometry is according to figure 11.

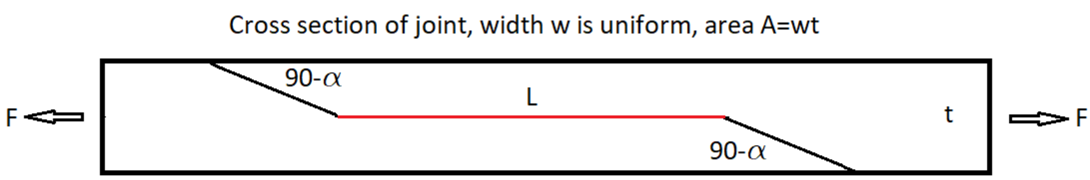

Figure 11: Cross section of scarf joint with additional step

The shear stress is,

$$\tau = \frac{F_T}{\sum A_{T_i}} = \frac{F\sin(\alpha)}{A_{T_1}+A_{T_2}}.$$

There are 2 surfaces $A_{T_1} = \frac{A}{\cos(\alpha)}$ and $A_{T_2} = A_1 \sin(\alpha)$. In this, the surface A_1 is tilted to be in line with the traverse force F_T.

We model that,

$$p = \frac{A_{T_2}}{A} = \frac{L}{t}.$$

This gives shear stress (τ),

$$\tau_\alpha = \frac{F}{A} \frac{\sin(\alpha)}{\frac{1}{\cos(\alpha)} + p \ \sin(\alpha)} = \sigma_x \frac{\sin(\alpha)}{\frac{1}{\cos(\alpha)} + p \ \sin(\alpha)} = \sigma_x \frac{1}{\tan(\alpha) + p} \ .$$

If the step in the center does not exist, $p \to 0$, then $\frac{\tau}{\sigma} = \frac{\sin(\alpha)}{\frac{1}{\cos(\alpha)}} = \frac{1}{2}\sin(2\alpha) = \frac{1}{\tan(\alpha)}$.

If the scarf does not exist but only the step, then $\alpha = 0$ and the solution for the scarf only is then $\frac{\tau}{\sigma_x} = \frac{\sin(\alpha)}{\frac{1}{\cos(\alpha)}} = \frac{1}{2}\sin(0) = 0$. The scarf with the step however is reducing to $\tau = \sigma_x \frac{1}{\tan(\alpha)+p} = \frac{\sigma}{p}$.

Normal stress is as same as in scarf joint model

$$\sigma_\alpha = \sigma_X \cdot \cos^2 \ \alpha$$

Strength of an adhesive joint under shear stress is a function of step length (L) to adherent thickness (t) ratio indicated by parameter (p). Shear stress on joint decreases as p increases i.e. longer step length increases joint strength.

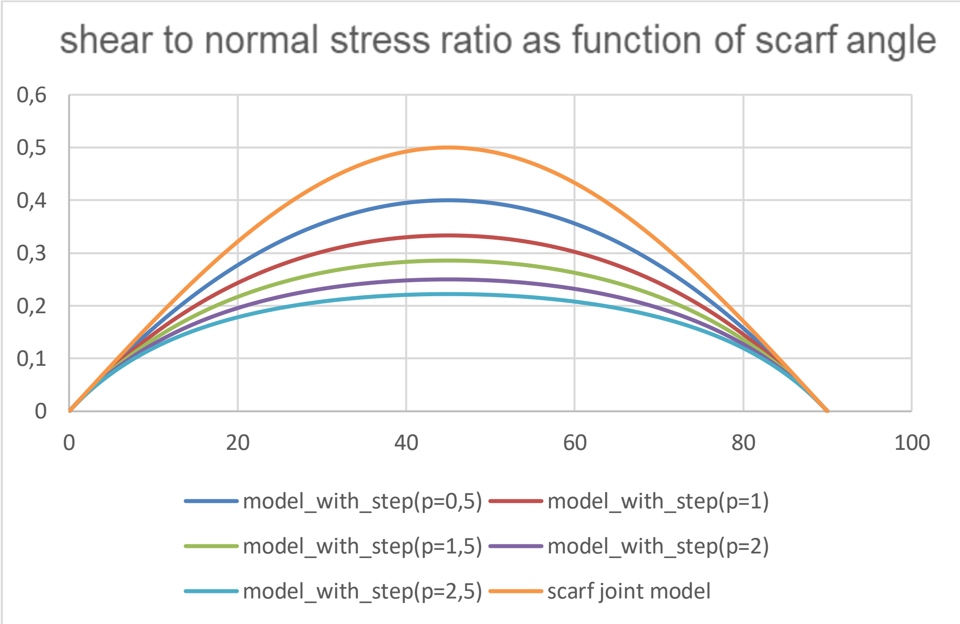

Figure 12: Step scarf joint shear to normal stress ratio

Figure 12, illustrates shear to normal stress ratio as function of scarf angle of 6 different joints. It is clear that step scarf joint are stronger than scarf joint where value of p is 0. On increasing value of p, step scarf joint strength also increases gradually as seen in graph. Hence, step scarf joint theory suggests to have longer step length in order to increase adhesive joint strength.

3.5 Shear stress distribution in bond line

Shear stress distribution in bond line is described by Volkersen and Klein model.

3.5.1 Volkersen model

Volkersen model for shear stress distribution is based on differential shear.

Maximum shear stress at the end of bond line is given by,

$$\tau_{Kmax} = \frac{F}{b}\sqrt{\frac{1}{2}\cdot\frac{1}{Et}\cdot\frac{G_k}{t_k}}$$

Where,

τ_{Kmax} = Shear stress peak

F = Force acting along joint

b = Joint breadth

E = Young's Modulus of laminate

G_k = Laminate Elastic Modulus

t_k = Joint thickness

3.5.2 Klein model

According to Klein model shear stress distribution in adhesive joint can be obtained by,

$$\omega = \lambda \cdot l_u = \sqrt{\frac{G_{KI}(E_1 \cdot t_1 + E_2 \cdot t_2)l_u^2}{E \cdot t_1 \cdot E_2 \cdot t_2 \cdot d}}$$

$$\beta = \frac{(E_2 \cdot t_2 - E_1 \cdot t_1) \cdot G_{KI} \cdot l_u^2}{E_1 \cdot t_1(G_{KI} \cdot l_u^2 + E_2 \cdot t_2 \cdot d)}$$

For symmetrical lap joints $\beta = 0$,

$$\tau_m = \frac{F}{l_u^2 \cdot b} \leq \tau_{zB}$$

$when\ x = 0;$ $$\tau_{max} = \omega \cdot \tau_m * \frac{sinh\omega}{(\beta+2)(cosh\omega-1)} = k'_\tau \cdot \tau_m$$

$when\ x = l_u;$ $$\tau_{max} = \omega \cdot \tau_m \cdot \frac{(\beta+1)sinh\omega}{(\beta+2)(cosh\omega-1)} = k''_\tau \cdot \tau_m$$

$$\tau_{max} = \tau_m \cdot k_\tau$$

3.5.3 Volkersen and Klein model analysis

Technical datasheet of an example sample is illustrated by table 1.

Table 1: Table showing sample technical datasheet

$E_1 = E_2$	70000	MPa
$t_1 = t_2$	2	mm
b	10	mm
d	0,1-2	mm
G_k	2000	MPa
F	100	N
l_u	3-40	mm

On increasing thickness of bond line from 0,1-2 (i.e. from 1% to 100% of bond line thickness to laminate thickness) we get following graphs showing the effect of decreasing shear stress on joint due to increased bond line thickness.

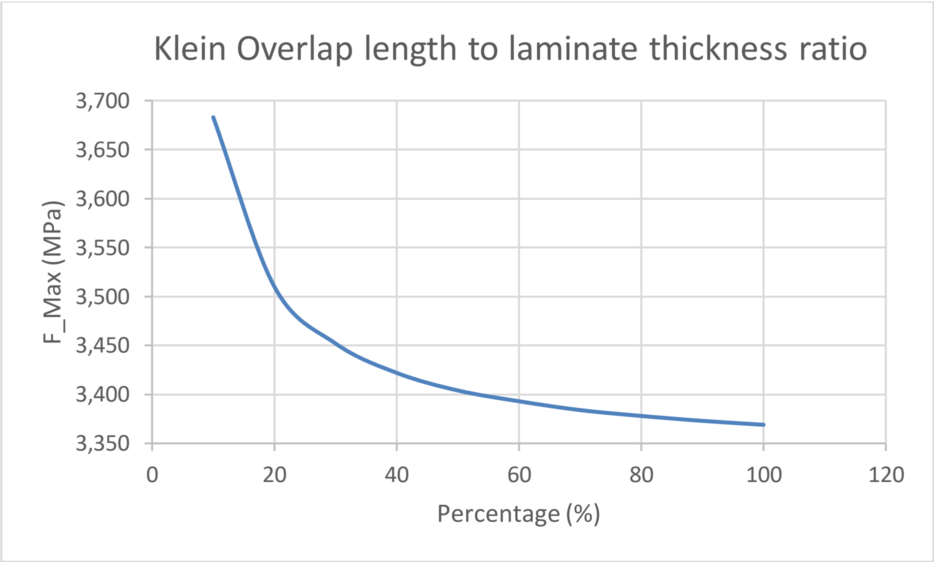

Figure 13: Klein model on increasing joint thickness to material thickness ratio.

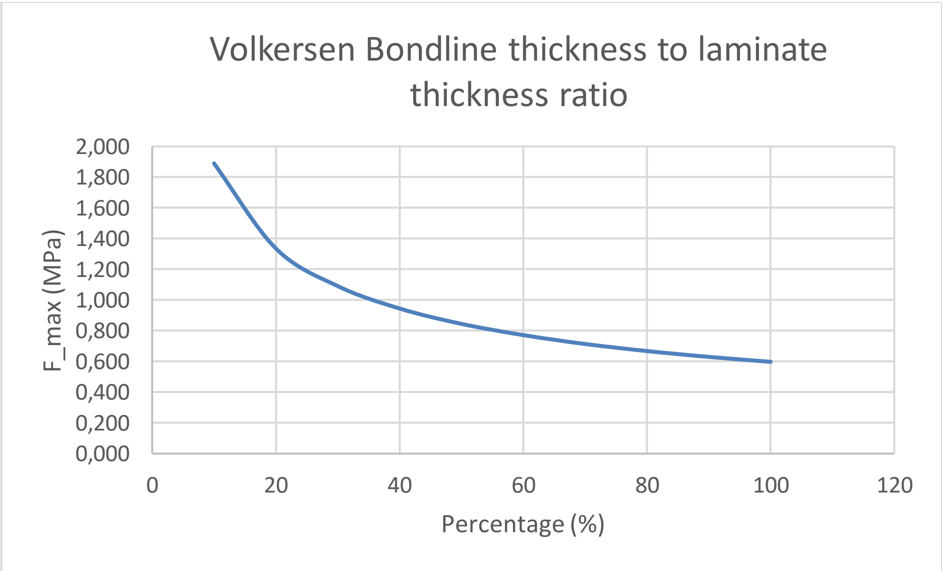

Figure 14: Volkersen model on increasing joint thickness to material thickness ratio

The Volkersen and Klein model shows that the thicker bond line reduces shear stress peaks at the edge and therefore delay the onset of peeling.

3.6 Three Point Bend Test

3 point bend test includes beam theory and force-displacement graph.

3.6.1 Beam theory

The three point bend test (figure 11) is a classical experiment in mechanics, used to measure the Young's modulus of a material in the shape of a beam. The beam, of length L, rests on two roller supports and is subject to a concentrated load P at its center. Figure also show graphs of bending moment M, shear Q and deflection w.

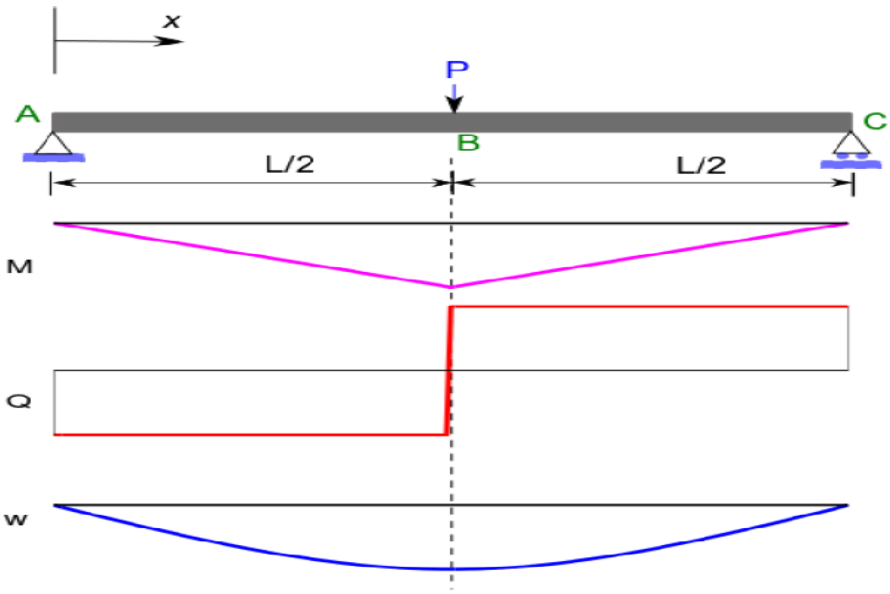

Figure 15: Schematic of the three point bend test. [15]

It can be shown that the deflection w_0 at the centre of the beam is

$$w_0 = \frac{PL^3}{48EI}$$

Where, E is the Young's modulus. I is the second moment of area defined by

$$I = \frac{t^3 b}{12}$$

Where, t is the beam's thickness and b is the beam's width. By measuring the central deflection w_0 and the applied force P, and knowing the geometry of the beam and the experimental apparatus, it is possible to calculate the Young's modulus of the material.

3.6.2 Force-displacement graph

If the applied force P is plotted against central displacement w_0, a straight line is obtained provided we remain within the elastic limit of the material (i.e. the beam returns to its original shape after deflection). The gradient of this line is,

$$\frac{dP}{dw_0} = \frac{48EI}{L^3}$$

For measuring E we can take several measurements of P and w_0, and deal sensibly with experimental error by finding a line of best fit from which we obtain the gradient $dP{=}dw_0$. There is also less need for calibration, since we only need to know changes in the measured values, not the actual values. [15]

3.7 Peel strength theory

Peel strength theory analyzes peeling strength per peel percentage value. Peel resistance of adhesives can be compared by this theory.

3.7.1 Peel stress at failure

Stress is in a cantilever beam is given by,

$$\sigma = \frac{FLc}{4I}$$

Where,

F is maximum force applied

L is beam's free length

c is half thickness of beam

$$I = \frac{1}{12}bh^3$$

b is beam's breadth, and

h is beam's thickness

3.7.2 Peel resistance

The motion of the beam is given by,

$$F = \frac{3EI}{L^3}\ \Delta x$$

Where,

E is beam's young's modulus

In case of this experiment, data $F(\Delta x)$ is not linear as it actually should have been (the reason is that L^3 increases due to peeling)

The procedure: Given data goes from 0 to 20mm before breaking. Take that region and divide it into 2 half.

Get the slope k_i from each section and integrate the $W = \int F\ dx$ for this regions. Results in 2 energies.

Calculate the energy difference, ΔW.

Given,

$$F \propto \frac{1}{L^3}$$

We get,

$$\frac{k_1}{k_2} = \left(\frac{L_2}{L_1}\right)^3$$

Where,

L_1 is the free length at the beginning

L_2 the new free length due to peeling.

Now,

Peeling progression Z is given by,

$$Z = \frac{L_2}{L_1} = \sqrt[3]{\frac{k_1}{k_2}}$$

And, peeling energy per peel percent, μ is given by,

$$\mu = \frac{\Delta W}{Z}$$

Hence, μ gives us Peel work per percent length increase.

4 METHOD/RESULT

This chapter includes experimental method for adhesive joint preparation, bonding and testing and result obtained after test data and sample analysis.

4.1 Materials used

Following materials were used during the test.

I. UD Glass fiber vinyl ester laminate of 6 plys with 1200 g/m^2 in each ply.

I. UD Glass fiber vinyl ester laminate of 8 plys with 1200 g/m^2 in each ply.

II. Atlac E-Nova MA 6215 Vinyl ester resin

Table 2: Atlac E-Nova MA 6215 Vinyl ester resin technical datasheet. [16]

Property	***value***	***unit***
Tensile strength	70	MPa
Tensile E-modulus	4	GPa
Elongation at break	2.maalis	%
Flexural E-modulus	4	GPa
Flexural strength	120	MPa

III. ARPOL^{TM} m 105 TB Polyester resin

IV. Peroxide Hardener

Table 3: Arpol TM 105 TB Polyester Resin Technical datasheet [17]

post-cure 24h at 50 °C		
property	***value***	***unit***
Tensile strength	55	MPa
Tensile Modulus	3600	MPa
Elongation at break	2	%
Flexural strength	90	MPa
Flexural Modulus	4100	MPa

V. West System 105 Epoxy Resin

VI. West System 206 Slow Hardener

Table 4: WS 105 Epoxy with WS 206 Hardener Technical datasheet [18]

Cured at room temperature for 2 weeks		
property	***value***	***unit***
Tensile strength	50,46	Mpa
Tensile Modulus	3,17	MPa
Elongation at break	4,5	%
Flexural strength	81,42	MPa
Flexural Modulus	3,1	MPa

VII. Loctite 435

VIII. Cellulose additive

IX. Silica additive

X. Microballs SG additive

XI. Phenol Microballs additive

XII. Glass fiber paste additive

XIII. Cocraft HBD Sanding Machine – 120 Grid sandpaper

XIV. Testometric Machine – M – 350 5CT

4.2 Test procedure

Glass fiber laminated with vinyl ester resin's specimen were prepared and bonded for adhesive joint strength testing.

4.2.1 UD Laminate

Vacuum laminated 6 and 8 layers of [0,90] orientated UD glass fiber with vinyl ester resin laminate were used as samples. Laminates had curing time of 24 hours during their lamination process.

Laminates were marked and cut using water jet, averaging width of 20 mm and length of 280 mm.

4.2.2 Laminate Joint preparation

Scaled UD laminates were marked and cut into halves using bandsaw. Then they were sanded on Cocraft HBD Sanding Machine with 120 Grid sand paper using a jig on desired angle. Figure 16 and figure 17 shows sanding process with jig support and sanded laminate sample of 86° scarf angle respectively.

Figure 16: Sanding process using jig

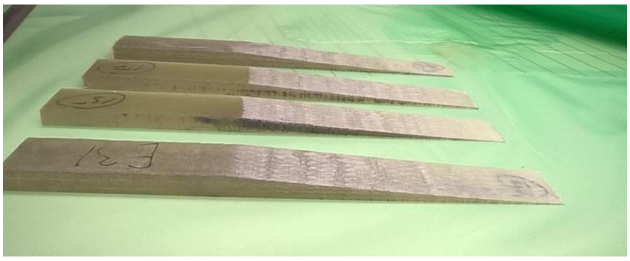

Figure 17: Sanded 86° scarf amgle UD laminate

4.2.3 Surface Treatment

It is important to make samples dust free prior to bonding. Sanded laminates were made dust free with pressurized air. Then they were rinsed in water and left for drying. Drying of laminates was done through heat gun or letting them to dry at normal temperature. It is important to dry the laminates properly to ensure proper surface bonding.

Prior to bonding laminates were rinsed with acetone. In some test prepared laminate surface were also subjected to 320 grid water sanding, ultrasonic cleaning, $NaOH$ treatment, H_2SO_4 treatment and HNO_3 treatment in some cases.

4.2.4 Bonding and testing

Bonding of UD laminate samples plays vital role in sample's test data. Hence, it is very important to maintain dimension stability while bonding process. Figure 18 shows samples bonding technique.

Figure 18: Bonding of scarf joint UD laminates

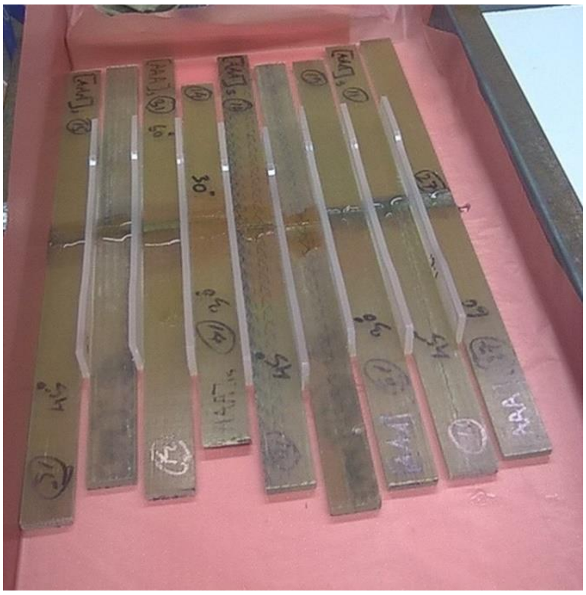

Samples were aligned such a way that the sample placed later on top would itself slide to its joining position with very less effort. Dimension stability of samples while bonding was maintained using plastic dog bone of equal dimension in between each sample. This ensured joined samples to be straight while placing them against straight metal support at one end while applying gentle force from other end. Each samples repeated similar process.

Excess adhesive were removed as much as it was possible. It is worthwhile to remove excess adhesive as much as possible in their uncured stage because they have to be removed by sanding after curing. Then, samples were subjected to 24 hours of curing time. Cured laminates were re-sanded to remove excess adhesive from cured samples. 3 point bending test and peel test as shown in figure 19 were performed on samples to get adhesive joint strength data and peel strength data respectively.

Figure 19: 3 point bending test (left) and Peel test (right)

4.3 UD Laminate (6 and 8 layer) bending strength

UD Laminate of 6 layer of ply and UD laminate of 8 layer of ply strength data were collected in order to get maximum achievable force on prepared adhesive joint. So that, each of data could exactly tell about their performance in comparison to original laminate strength.

3 Samples of scaled UD laminates (6 ply) and 2 samples of scaled UD laminate (8 ply) were subjected to 3 Point Bending Test in Testometric Machine M – 350 5CT with testing length of 160 mm. Peak Force (F_max) data were obtained from test. Then, stress on the laminate was calculated.

Data obtained from the test are listed in table 5 and table 6 below,

Table 5: UD laminate (6 ply) bending strength data

Sample	Width (mm)	Thickness (mm)	Length (mm)	F_{max} (N)	Stress (MPa)
UD laminate (6 layer ply)	20,00	5,40	160,00	2204,90	907,37
	20,20	5,50	160,00	2421,70	951,16
	20,20	5,40	160,00	2630,70	1071,87

From the data, average stress of laminate is $976{,}80\ MPa$ and maximum force applied is $2630{,}7\ N$.

Table 6: UD laminate (8 ply) bending strength data

Sample	Width (mm)	Thickness (mm)	Length (mm)	F_{max} (N)	stress (MPa)
UD laminate (8 ply)	25,00	7,80	160,00	5039,40	795,17
	25,00	7,90	160,00	5031,80	774,00

From the data, average stress of laminate is $784{,}58\ MPa$ and maximum force applied is $5039{,}4\ N$.

4.3.1 Result

Outcome based on the test result shows that UD Glass fiber laminate possess good amount of strength and can be used in many areas. These are the data collected for comparative study later.

4.4 Joints strength as function of angle

30°, 45° and 60° scarf angle on adhesive joint in UD laminate were joined by resin as adhesive in this test. Motivation for this experiment was to study how joint strength varies due to scarf angle and due to resin or adhesive. This test was also subjected to see if the primary resin used for lamination would have impact while bonding them again with similar resin.

4.4.1 30°, 45° and 60° scarf angle

9 Samples of UD laminates were cut into two halves by Bandsaw after marking them properly. Then, Laminates were sanded on 30°, 45° and 60° scarf angles. After, making the laminates dust free they were bonded using polyester, vinyl ester and epoxy as adhesive.

Peak Force (F_max) were obtained from test and stress was calculated.

Data obtained from the test are listed in table 7 below,

Table 7: 30°, 45° and 60° scarf angle strength data

Adhesive	*Angle (°)*	F_{max} *(N)*	*Width (mm)*	*Thickness (mm)*	*Length (mm)*	*Stress (Mpa)*
Polyester	30,00	108,90	20,00	5,50	160,00	43,20
	45,00	130,25	20,00	5,00	160,00	62,52
	60,00	148,65	20,00	5,10	160,00	68,58
Epoxy	30,00	116,50	20,00	5,40	160,00	47,94
	45,00	130,60	20,10	5,20	160,00	57,67
	60,00	160,23	20,10	5,50	160,00	63,25
Vinyl ester	30,00	0,00	19,90	5,30	160,00	0,00
	45,00	0,00	20,00	5,30	160,00	0,00
	60,00	80,20	20,00	5,50	160,00	31,81

Data from obtained from this test shows gradual increase in joint stress as scarf angle of joint increases. Stress for polyester and Epoxy adhesive is minimum at 30° scarf angle, while maximum at 60° scarf angle.

Adhesive joints were not completely filled due to adhesives being less viscous and running away from joint due to steep angles. To avoid adhesives running away, viscosity of adhesives must be increased. Likewise, scarf joint angle also must be increased.

4.4.1.1 Result

Outcome based on the result of the test shows that adhesive joint strength increases as a function of angle. Vinyl ester possessing low viscosity wasn’t able to join properly on steep scarf angles. Hence, larger scarf angles required for less viscous adhesives while bonding. Prior to adhesive bonding, bonding surface must be primed to ensure proper adhesive bonding.

4.4.2 60°, 70° and 80° scarf angle

Experiment includes strength data for UD laminate joined by Epoxy resin as adhesive at 60°, 70° and 80° scarf angle adhesive joint. Motivation for this experiment was also to study how joint strength increases on increasing scarf angle. This test was also subjected to see how priming initially with same resin helps on joint surface bonding.

Data obtained from the test are listed in table 8 below,

Table 8: 60°, 70° and 80° scarf angle Epoxy strength data

Adhesive	***Angle (°)***	***Width (mm)***	***Thickness (mm)***	***length (mm)***	F_{max} ***(N)***	***Stress (MPa)***
WS 105 Epoxy	60,00	20,00	5,50	160,00	295,86	117,37
	70,00	20,00	5,00	160,00	408,95	196,30
	80,00	20,00	5,00	160,00	665,50	319,44

Maximum force applied is $665{,}5\ N$ at 80° scarf angle having stress of $319{,}44\ MPa$. Data shows gradual increase in stress due to increasing scarf joint angle.

4.4.2.1 Result

Outcome based on the test result shows that greater scarf angle resulted in stronger adhesive joint. Hence, confirming scarf joint theory. Observation of test samples indicated that viscosity of resin in joint must be increased for proper bonding and initial priming of bonding section improved adhesive bonding.

80° scarf angle on adhesive joint was able to achieve $\mathbf{32{,}70\%}$ ***of laminate's original strength***.

4.5 Joint strength as function of adhesive

Test includes strength data for UD laminate joined by Epoxy resin as adhesive at 80° scarf angle. Motivation for this experiment was to study and compare which adhesive performs best at strength. Adhesive breakage after bending test has also been studied in this test.

Previously used samples were re-sanded on 80° scarf angle and more new samples were prepared. Vinyl ester resin, polyester resin, Loctite 435 and WS 105 epoxy resin was used as adhesive. Each sample were primed with respective adhesive resin prior to bonding.

Data obtained from the test are listed in table 9 below,

Table 9: Strength data for 80° scarf angle

Adhesive	***Angle (°)***	F_{max} ***(N)***	***Width mm)***	***Thickness (mm)***	***Length (mm)***	***Stress (MPa)***	***Average stress (MPa)***	F_{max} ***(N)***
Vinyl ester	80,00	534,60	20,00	5,00	160,00	256,61	192,22	534,60
	80,00	325,20	20,00	5,00	160,00	156,10		
	80,00	432,40	20,00	5,00	160,00	207,55		
	80,00	309,60	20,00	5,00	160,00	148,61		
Polyester	80,00	277,60	20,00	5,00	160,00	133,25	163,70	395,30
	80,00	345,16	20,00	5,00	160,00	165,68		
	80,00	346,11	20,00	5,00	160,00	166,13		
	80,00	395,30	20,00	5,00	160,00	189,74		
Loctite 435	80,00	858,20	20,00	5,50	100,00	212,78	230,27	858,20
	80,00	503,95	20,00	5,00	160,00	241,90		
	80,00	558,30	20,00	5,00	160,00	267,98		
	80,00	504,30	20,00	5,20	160,00	223,80		
	80,00	476,90	20,00	5,00	160,00	228,91		
	80,00	429,73	20,00	5,00	160,00	206,27	242,74	680,00
WS 105 Epoxy	80,00	440,40	20,00	5,50	160,00	174,70		
	80,00	406,00	20,00	5,00	160,00	194,88		
	80,00	579,00	20,00	5,00	160,00	277,92		
	80,00	650,00	20,00	5,20	160,00	288,46		
	80,00	480,30	20,00	5,00	160,00	230,54		
	80,00	680,00	20,00	5,00	160,00	326,40		

Average stress at 80° scarf joint angle achieved by WS 105 Epoxy resin is 242,74 MPa ***(24,85% of laminate's original strength)**, vinyl* ester resin is 192,22 MPa ***(19,68% of laminate's original strength),*** polyester resin is 163,7 MPa ***(16,76% of laminate's original strength)*** and Loctite 435 is 230,27 MPa ***(23,57% of laminate's original strength).***

4.5.1 Result

WS 105 Epoxy resin proved to have strongest bonding. Vinyl ester performance as adhesive is better than polyester. Average stress for WS 105 epoxy is less than previous stress.

Observation of adhesive joint breakage clarified that scarf angle must be increased to achieve higher strength. Since, joints failure mode was due to simply not having enough adhesive between bonds viscosity of adhesive should be increased by additives.

4.6 Joint strength as function of additives in adhesives

Motivation for this experiment is to see how additives effects joint stress by increasing viscosity of adhesive. Therefore, increasing adhesive bond line thickness.

4.6.1 60°, 70° and 80° scarf angle with additives strength

Cellulose and silica additives effects are studied by mixing them with polyester and vinyl ester resin at 60°, 70° and 80° scarf joint angle.
Cellulose and silica additives were mixed with polyester and vinyl ester resin to create viscous additive paste which increased the viscosity of adhesive. Mixing has been done in an increasing order for resin to avoid air bubble and lumps.
It is important to note that additive paste should be enough viscous to stay at the joint and enough paste should be applied to joint surface prior to bonding.
Data obtained from the test are listed in table 10 below.

Table 10: Joint strength at 60°, 70° and 80° scarf angle with additives

Adhesive	***Angle (°)***	F_{max} ***(N)***	***Width (mm)***	***Thickness (mm)***	***Length (mm)***	***Stress (MPa)***
Polyester + Cellulose	60,00	264,00	20,00	5,50	160,00	104,73
	70,00	331,70	20,00	5,00	160,00	159,22
	80,00	563,00	20,00	5,00	160,00	270,24
Polyester + Silica	60,00	242,55	20,00	5,50	160,00	96,22
	60,00	203,42	20,00	5,00	160,00	97,64
	70,00	240,20	20,00	5,10	160,00	110,82
Vinyl ester + Cellulose	60,00	314,30	20,00	5,40	160,00	129,34
	70,00	355,00	20,00	5,10	160,00	163,78
	80,00	589,70	20,10	5,20	160,00	260,40
Vinyl ester + Silica	80,00	430,36	19,90	5,30	160,00	184,77
	70,00	251,17	20,00	5,30	160,00	107,30
	80,00	869,10	20,00	5,50	160,00	344,77

At 80° scarf angle, polyester with cellulose additive joint strength increased by 39,42% compared to samples without additive and achieved $\mathbf{27,67}$% ***of laminate's original strength***, vinyl ester with silica additive joint strength increased by 44,26% and achieved ***(*** $\mathbf{27,11}$% ***of laminate's original strength)*** while vinyl ester with cellulose additive joint strength increased by 26,19% and achieved ***(*** $\mathbf{26,66}$% ***of laminate's original strength)***. However, test samples showed poor wetting of adhesive joint interface surfaces.

4.6.1.1 Result

Samples showed increase in joint stress on adding additives. Initial priming of surface prior to adhesive bonding is essential as broken samples showed co-adhesive breakage.

4.6.2 Joint strength at 80° scarf angle with additives

This test highlights on adhesive joint strength of cellulose, silica, phenol microballs, microball SG and glass fiber paste additive as a function of WS 105 Epoxy resin on 80° scarf joint angle.

Epoxy was able to achieve highest strength on previous test. Hence, it has been used as base resin.

Data obtained from the test are listed in table 11 below,

Table 11: 80° scarf angle with additives joint strength

Additive	***Angle (°)***	F_{max} ***(N)***	***Width (mm)***	***Thickness (mm)***	***length (mm)***	***Stress (MPa)***	***Average stress (MPa)***	F_{max} ***(N)***
Glass fiber paste	80,00	360,12	20,00	5,50	160,00	142,86	210,11	564,00
	80,00	564,00	20,00	5,00	160,00	270,72		
	80,00	451,56	20,00	5,00	160,00	216,75		
Phenol microballs	80,00	389,60	20,00	5,20	160,00	172,90	207,15	530,50
	80,00	530,50	20,00	5,00	160,00	254,64		
	80,00	404,00	20,00	5,00	160,00	193,92		
Cellulose	80,00	638,60	20,00	5,10	160,00	294,63	265,98	638,60
	80,00	605,20	20,00	5,20	160,00	268,58		
	80,00	489,00	20,00	5,00	160,00	234,72		
Microballs SG	80,00	312,13	20,00	5,00	160,00	149,82	161,25	341,48
	80,00	333,33	20,00	4,95	160,00	163,25		
	80,00	341,48	20,00	4,90	160,00	170,67		
Silica	80,00	590,00	20,00	4,85	160,00	300,99	272,09	590,00
	80,00	475,00	20,00	4,80	160,00	247,40		
	80,00	503,70	20,00	4,75	160,00	267,90		

Average adhesive joint strength in comparison to only using WS 105 Epoxy as adhesive at 80° scarf angle for WS 105 Epoxy with Glass fiber paste additive decreased by 16,54% and achieved $\mathbf{21,51}\%$ ***of laminate's original strength***, with phenol microballs additive decreased by 17,55% and achieved $\mathbf{21,21}\%$ ***of laminate's original strength***, with cellulose additive increased by 5,7% and achieved $\mathbf{27,23}\%$ ***of laminate's original strength***, with microballs SG decreased by 35,92% and achieved $\mathbf{16,51}\%$ ***of laminate's original strength***, and with silicon additive by 8,12% and achieved $\mathbf{27,86}\%$ ***of laminate's original strength***.

4.6.2.1 Result

Silica and cellulose additive showed increase strength at adhesive joint, also increasing viscosity of adhesive paste created. While, microballs SG, phenol microballs and glass fiber paste only increased viscosity but had negative effect on strength.

Initial priming of joint interface surface helped in adhesive bonding as breakage samples showed strong adhesive bonding.

4.7 Initial surface treated 85° scarf joint strength

Motivation for this experiment was to see how initial surface treatment effects joint stress. For this experiment 4 samples of laminate were assembled at 85° scarf joint angle, all possessing WS 105 Epoxy with Cellulose as additive in adhesive joints.

4 pair of samples were re-sanded in 85° scarf angles and were subjected to surface treatment procedure given in table 12.

Table 12: Initial surface treatment process

Sample	***(1st step)Initial treatment***	***(2nd step)Ultra-sonic bath in H_2O for 15 min***	***(3rd step)Dried in oven for 45 min at 75 °***
Sample 1	No treatment	yes	yes
Sample2	$NaOH$ treatment (1h @ 50°C gentle stirring) and rinse with tap water	yes	yes
Sample 3	H_2SO_4 treatment (1h @ 50°C gentle stirring) and rinse with tap water)	yes	yes
Sample 4	HNO_3 treatment (1h @ 50°C gentle stirring) and rinse with tap water)	yes	yes

HNO_3 treatment burned sample surface a bit and had faint yellow color on interface surface. After, surface treatment procedure samples were bonded and subjected to 3 point bending test.

Following data was obtained after the test.

Table 13: strength data for initially surface treated samples

Adhesive	***Angle (°)***	***Thickness (mm)***	***Width (mm)***	***length (mm)***	***F_{max} (N)***	***Stress (MPa)***
sample 1	85,00	7,30	25,00	160,00	3036,90	182,36
sample 2	85,00	7,80	25,00	160,00	2838,80	149,31
sample 3	85,00	7,90	25,00	160,00	2899,90	148,69
sample 4	85,00	7,40	24,90	160,00	1177,40	69,08

Sample 1 achieved $\mathbf{23,24\%}$ ***of laminate's original strength***, sample 2 achieved $\mathbf{19,03\%}$ ***of laminate's original strength***, sample 3 achieved $\mathbf{18,95\%}$ ***of laminate's original strength*** and sample 4 achieved $\mathbf{8,8\%}$ ***of laminate's original strength***.

4.7.1 Result

Sample treated in ultrasonic bath with H_2O for 15 min and then dried in oven for 45 min at 75° had best strength. There was no prior chemical surface treatment before ultrasonic bath like in rest of samples. Sample treated with HNO_3 showed low strength as acid rotted bonding surface partially.

Partial cohesive breakage of adherent was observed.

4.8 Peel strength

Peel strength experiment is subjected towards finding peeling energy per peel percent. This clarifies which bond is more peel resistance.
Experiment includes strength data for UD laminate bonded by Vinyl ester, Poly ester, WS 105 Epoxy, WS 105 Epoxy + Cellulose fiber and WS 105 Epoxy + Silicon.
Motivation for this experiment is to find peel energy per peel Percent. Test is also subjected in finding which of the adhesive used gives strongest peel resistance bond.

4.8.1 Test Procedure

UD laminate samples were taken and cut into halves with equal length. Metal strip with L shape, were attached to one end of samples using Loctite 435 then the samples were let to be dried for a day. Figure 20 indicates peel test samples preparation process.

Figure 20: Preparation of peel test samples

4.8.1.1 Surface treatment

Laminates were made dust free with pressurized air. Then laminates were rinsed in water and let it to be dry and were cleaned with acetone prior to bonding.

4.8.1.2 Bonding

Vinyl ester resin, Polyester resin, WS 105 Epoxy resin, WS 105 Epoxy resin with Cellulose additive and WS 105 Epoxy resin + Silicon additive has been used as adhesive. Each sample were primed with respective adhesive resin prior to bonding.

Samples were bonded such that adhesive bonding was applied on one edge with vacuum foil placed in between, creating a bond line towards other edge and all of the samples having equal weight on top. Samples were subjected to 24h curing at room temperature.

4.8.1.3 Testing

Cured laminate were removed from laminating table and sanded on sanding machine so that no excess adhesive remains on the joints i.e. matching samples initial profile. Laminates were subjected to peel test in Testometric Machine M – 350 5CT with testing length of 160 mm.

Force and displacement data were obtained from test and these data were then calculated according to peel strength test theory.

4.8.2 Test Data Analysis Method

Following steps show process of calculation of μ for Epoxy peeling,

I. 1st we take displacement vs Force data, we get maximum force from data.

II. Then we calculate peel stress. Given in table below,

Parameter	***Value***	***Unit***
t	4,00	mm
b	20,00	mm
l_1	113,00	mm
F_{Max}	40,74	N
I	106,67	mm^4
σ_{Max}	21,58	MPa

Table 13: Maximum peel stress for Epoxy peeling

III. 2 graphs shown in figure 21 and figure 22 are to be created. 1st being displacement until maximum force and 2nd being displacement until half of maximum force applied.

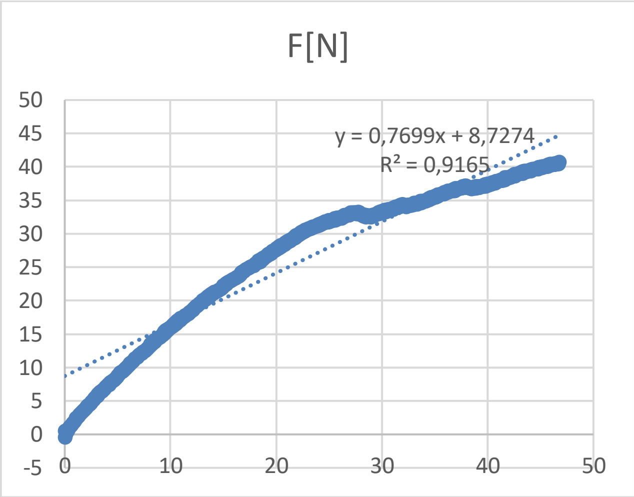

Figure 21: Epoxy peeling full curve.

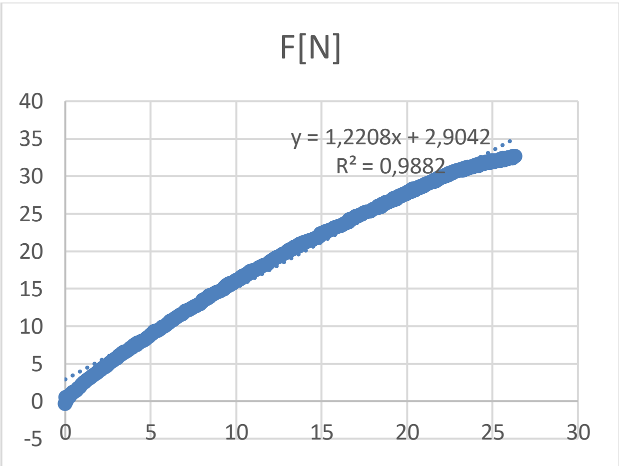

Figure 22: Epoxy peeling half curve.

IV. Then slopes were taken from graph and peel resistance calculated as in table below,

Table 14: Peel energy per peel % calculation

Parameter	***Value***	***Unit***
W_1	1,33	mJ
W_2	1,59	mJ
dW	1,22	mJ
k_1	1,22	N/mm
k_2	0,79	N/mm
z	1,17	no unit
µ	0,19	no unit

Hence, Peel energy per Peel % in Epoxy peeling is 0,19

4.8.3 Peel strength data

3 sets of data for each case was obtained and then finalized into single average for each samples. Data obtained from test are illustrated in table 15.

Table 15: Average μ(peel energy/peel %) for adhesives

Adhesive	***Average μ (Peel energy/peel %)***
WS 105 Epoxy + cellulose	0.25
WS 105 Epoxy + Silica	0.30
WS 105 Epoxy	0.19
Vinyl ester	0.28
Polyester	0.15

4.8.4 Result

Peel strength data analysis shows WS 105 Epoxy with Silica and Cellulose additive adhesive bonding material has higher peel resistance. Hence, additives are very influential in increasing peel resistance comparing to only resin (like WS 105 Epoxy, Polyester) being used as adhesives.

Vinyl ester however, bonded properly and possessed high peel resistance. This is due to its viscous nature and also as initial laminate was laminated with vinyl ester resin.

4.8 Step scarf joint strength

Experiment includes strength data for WS 105 Epoxy resin mixed with cellulose, silica and phenol microballs as additives on step scarf joint.

Due to sanding machine and time limitation, simpler profile shown in figure below of step scarf joint was used.

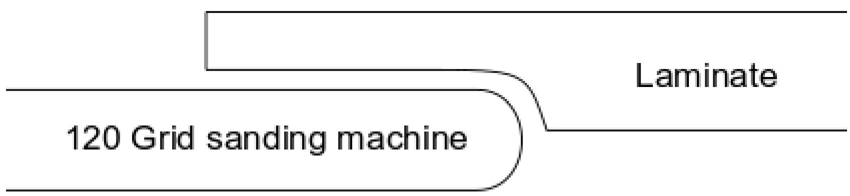

Figure 23: Laminate's profile for step scarf joint

Similar test procedure was followed on 9 pair of samples.

Following data were obtained after 3 point bending test.

Table 16: Step scarf joint strength data.

Adhesive	***Thickness (mm)***	***Width (mm)***	***Length (mm)***	F_{Max} ***(N)***	***Stress (MPa)***	***Average stress*** (MPa)	F_{Max} ***(N)***
Epoxy + cellulose 1	8,20	24,90	160,00	677,70	97,15	100,42	764,20
Epoxy + cellulose 2	7,75	24,75	160,00	494,00	79,76		
Epoxy + cellulose 3	7,56	24,94	160,00	533,70	89,86		
Epoxy + cellulose 4	7,41	24,76	160,00	764,20	134,91		
Epoxy + Phenol 1	8,25	24,95	160,00	337,88	47,75	81,25	99,03
Epoxy + Phenol 2	7,65	25,09	160,00	593,20	96,96		
Epoxy + Phenol 3	7,53	24,91	160,00	582,80	99,03		
Epoxy + Silica 1	8,10	24,79	160,00	519,70	76,69	74,95	712,40
Epoxy + Silica 2	8,44	24,93	160,00	290,26	39,23		
Epoxy + Silica 3	8,00	25,02	160,00	394,00	59,05		
Epoxy + Silica 4	7,42	24,88	160,00	712,40	124,82		

Average stress for at step scarf joint for WS 105 Epoxy with Cellulose additive is 100,42 MPa and achieved ***12,8% of laminate's original strength***, while phenol microballs additive is 81,25 MPa and achieved ***10,36% of laminate's original strength*** and silica additive is 74,95 MPa and achieved ***9,55% of laminate's original strength***.

4.8.2 Adhesive joint breakage

All the breakage were due to co-adhesive failure but partial cohesive failure is also observed as on figure 24, figure 25 and figure 26. Due to low peel resistance on adhesives breakage started at joint tips.

Cellulose additive as shown in figure 24 was able to bond with joint surface fibers. Hence, having highest average stress and comparatively more cohesive breakage (indicated by white parts on joining interface of samples).

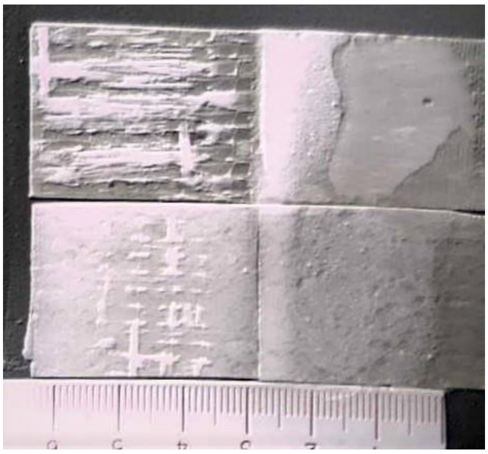

Figure 24: Co-adhesive failure in step scarf joint (cellulose)

Phenol microballs additive were partially able to bond with joint surface fibers as seen in in figure 25. Hence, co-adhesive breakage dominates joint interface region in this case.

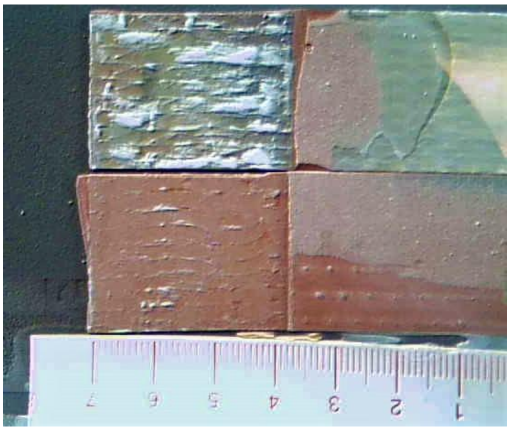

Figure 25: Co-adhesive failure in step scarf joint (phenol microballs)

Silicon additive performed the least only partially bonding with surface as seen in figure 26. Here also. Co-adhesive breakage dominates joint interface region.

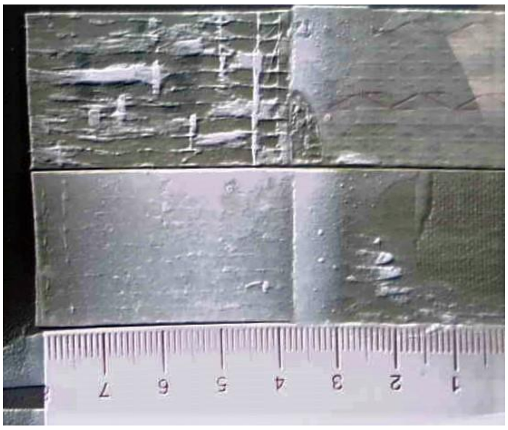

Figure 26: Co-adhesive failure in step scarf joint (Silica)

4.8.3 Result

All the breakage were due to insufficiency of adhesive to bond with bonding surface properly also known as ***Co-Adhesive bond breakage.*** Cellulose additive as seen in Figure 25, is better that phenol microballs and silica additive in co-adhesive bonding.
Breakage actually started due to peeling nature that started at the joint end and followed towards center of joint as described by strength due to bond line thickness in Volkersen and Klein Model.

4.9 86° scarf joint

In order to create high strength adhesive joint, 86° scarf angle joints were bonded using cellulose and silica additive with WS 105 Epoxy resin as adhesive.
3 UD laminate (8 ply) samples were bonded with epoxy with cellulose additive whereas 2 similar laminate were bonded with epoxy with silica additive.
Data obtained from the test is mentioned in table 19,

Table 17: Strength data for 86° scarf joint

Adhesive	***Thickness (mm)***	***Width (mm)***	***Length (mm)***	F_{Max} ***(N)***	***Stress (MPa)***	***Average stress (MPa)***	F_{Max} ***(N)***
Epoxy + cellulose 1	7,30	24,93	160,00	1791,00	323,55	242,18	1956,60
Epoxy + cellulose 2	7,81	24,91	160,00	669,00	105,67		
Epoxy + cellulose 3	7,95	24,99	160,00	1956,60	297,31		
Epoxy + Silica 1	8,10	24,90	160,00	1126,30	165,46	197,53	1301,80
Epoxy + Silica 2	7,40	24,85	160,00	1301,80	229,60		

Cellulose and silica additive with WS 105 Epoxy at 86° scarf angle created very strong joint. Average stress in cellulose bond is 242,18 MPa and it achieved $\mathbf{30,87}$% ***of laminate's original strength***, while in silica is 197,53 MPa *and it achieved* $\mathbf{25,18}$% ***of laminate's original strength***.

4.9.2 Joint failure mode

Adhesive joint breakage were due to co-adhesive, cohesive and adhesive breakage as seen in figure 27 and figure 28. In some parts bond was so strong that glass fiber laminate itself underwent cohesive failure.

Figure 27 is cellulose additive sample mixed with epoxy resin. Here, both additive breakage and adherent breakage can be observed. Thus implying, joint to be stronger than material itself.

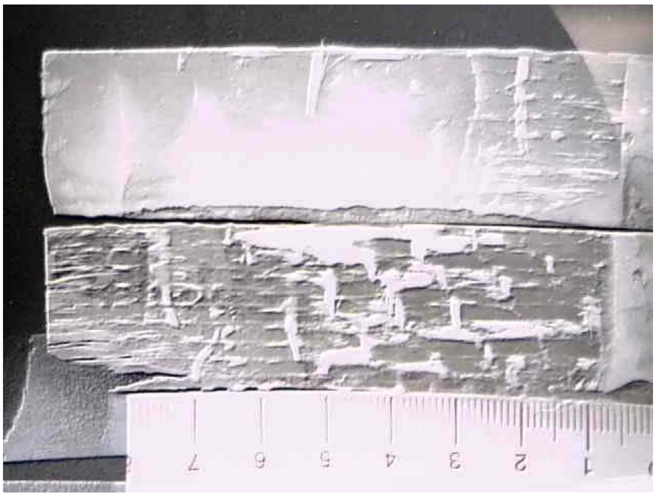

Figure 27: Co-Adhesive failure at 86° scarf angle (cellulose)

Figure 28 with silica additive, also shows additive and adherent breakage. Comparing to figure 27 it can be observed that scarf joint co-adhesive bond is stronger in figure 28.

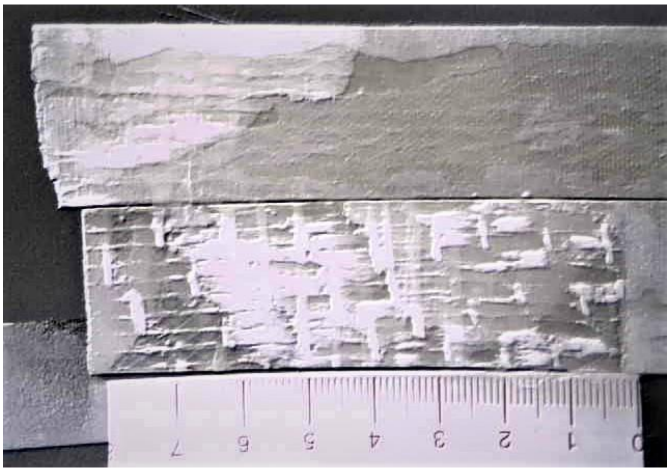

Figure 28: Co-Adhesive failure at 86° scarf angle (silica)

4.9.3 Result

Cohesive failure in adherent showed that adhesive scarf bond was stronger than adherent itself**.** Larger angle created larger contact surface area for bonding. Hence, resulting in increased strength at bond line.

Laminate itself was delaminated on edge due to excess adhesive bond strength. In order to avoid delamination, it is wiser idea to produce taper end at joint with enough additive as explained by strength due to bond line thickness in Volkersen and Klein Model.

5 CONCLUSION

The basic idea of this thesis work is to experimentally analyze adhesive joint strength data on adhesive scarf joints in order to see how adhesive bond strength changes as function of scarf angle, adhesives, additive in adhesives and Initial surface treatment. Further, adhesive joint strength as function of initial surface treatment, adhesive peel strength and step scarf joint has also been studied along with adhesive joint failure. Adhesive strength test and peel test were performed by 3 point bending test and peel strength test respectively.

The conclusion of this thesis work are based on test procedure and test data analysis.

Larger scarf angles with precise scarf angle can be created by using jig on sanding machine. Prior to adhesive bonding, samples must be dust free as it will lead to co-adhesive failure. One of the main conclusion is that the scarf joint interface must be primed initially with base resin while using additives.

Adhesive should be enough viscous for it not to run out from joint while bonding. Viscosity in adhesive can be increased by adding additives. The mixing process of additives in base resin should be thorough and in increasing order for adding resin to avoid air bubbles and lumps.

It is also concluded that geometry must be maintained while joining samples, different shape gives different strength data and proper curing of adhesive bond is vital for proper experimental data. For safety purpose proper disposal of excess resin while curing is important for not causing fire hazards. Cured laminate samples should be carefully sanded to get excess adhesives removed from the joint. Excess adhesives increases adhesive joint strength so, actual adhesive joint strength data can't be obtained.

Manually building L shaped metal strips and gluing them to laminate samples for peel test didn't ensure geometric similarities between all samples. Therefore, it would have been better idea to have hinges on laminate samples.

One of the main conclusion obtained for this study is about scarf joint theory. Which emphasizes on stronger adhesive joint strength on increasing scarf angle is proven to be true by test. WS 105 Epoxy resin gives stronger adhesive bond than Polyester, Vinyl ester and Loctite 435. It is also concluded that Cellulose and Silica as additive increases adhesive viscosity and bond strength, while Phenol Microballs, Glass fiber paste and Microball SG only increases viscosity. Cellulose and silica additive in epoxy also provides better peel resistance than epoxy itself and polyester resin. It is also recommended to do initial surface treatment in sample in ultrasonic bath with H_2O for 15 min and then drying in oven for 45 min at 75°C before bonding in order to clear joint interface with dust.

One of the most important conclusion of this study is, it is possible to create a scarf joint which is stronger than the adherent itself. As shown by comparative test data, $30{,}87\%$ of laminate's original strength was able to recover at 86° scarf angle joined by epoxy and cellulose as additive. Although this was highest achieved strength, it was enough to break adherent itself.

The other important conclusion is, in order to reduce peeling effect on scarf joint edges, they should be tapered prior to bonding as explained by adhesive joint strength due to bond line in Volkersen and Klein theory.

During 3 point bending test, samples must be placed such that the force acting should be in middle of joint. This ensures proper similar data. 4 point bending test would have been better instead of 3 point bending test as it enforces constant stress distribution on scarf joints. Likewise in peel strength test, cyclic peel test would have been better as it shows progression of peeling.

6 REFERENCES

[1] A. Q. M. A. M. J. A. M. J. L. B. V. D. Pedro Galvez, "Stuudy of the behaviour of adhesive joints of steel with CFRP for its application in bus structures," 15 11 2017. [Online]. Available: https://www.sciencedirect.com/science/article/pii/S1359836817315834. [Accessed 04 06 2018].

[2] S. E. a. C. Ebnesajjad, Surface Treatment of Materials for adhesive bonding, Elsevier science and Technology, 2013.

[3] "Adhesive Technology," [Online]. Available: https://webmail.arcada.fi/roundcube/?_task=mail&_framed=1&_frame=1&_mbox=INBOX&_uid=120&_part=4&_action=get&_extwin=1. [Accessed 25 05 2018].

[4] "Adhesives.org," [Online]. Available: http://www.adhesives.org/adhesives-sealants/science-of-adhesion/design-of-adhesives-bonds/types-of-adhesives. [Accessed 8 4 2018].

[5] www.huntsman.com, "Advanced Materials Araldite adheisves," [Online]. Available: http://www.huntsman.com/advanced_materials/Media%20Library/a_MCED5570E284BD76EE040EBCD2B6B7A1B/Your%20Industry_MCEFD19E1A181BDB8E040EBCD2B6B77C9/Marine_MD0AB2CDC727E93DBE040EBCD2C6B1FB1/files/SELECTOR%20GUIDE%20Adhesives%20Araldite%C2%AE%202000plus%20rang. [Accessed 25 05 2015].

[6] "Adhesives.org," [Online]. Available: http://www.adhesives.org/adhesives-sealants/fastening-bonding/fastening-overview/adhesive-bonding. [Accessed 8 4 2018].

[7] HUNTSMAN, "Araldite industrial adhesives," [Online]. Available: http://us.aralditeadhesives.com/files/USER-GUIDE_Adhesives-technology.pdf. [Accessed 30 05 2018].

[8] I. H. Andrew J. Gunnion, "Parametric study of scarf joints in composite structures," *Composite Structures,* vol. 75, no. 1-4, pp. 364-376, 2006.

[9] "Adhesives.org," [Online]. Available: http://www.adhesives.org/adhesives-sealants/science-of-adhesion/adhesion-cohesion. [Accessed 8 4 2018].

[10] www.astm.org, "Adhesive Standards," [Online]. Available: https://www.astm.org/Standards/adhesive-standards.html. [Accessed 25 05 2018].

[11] www.iso.org, "Standards Catalogue 83.180 Adhesives," [Online]. Available: https://www.iso.org/obp/ui/#iso:std:iso:4587:ed-3:v1:en. [Accessed 25 05 2018].

[12] www.astm.org, "Adhesive standards," [Online]. Available: https://www.astm.org/Standards/adhesive-standards.html. [Accessed 25 05 2018].

[13] C. W. a. A. Gunnion, "Desing Methodology for Scarf Repairs to Composite Structures," [Online]. Available: http://citeseerx.ist.psu.edu/viewdoc/download?doi=10.1.1.595.3351&rep=rep1&type=pdf. [Accessed 04 06 2018].

[14] Fachhochschule Nordwestschweiz Hochschule fur Technik, "Advanced Composites," *Krafteinleitungen: Klebeverbindungen (Schurmann Kap. 23 / Klein Kap. 22.4).*

[15] "The three point bend test," [Online]. Available: http://mi.eng.cam.ac.uk/IALego/bender_files/bend_theory.pdf. [Accessed 21 05 2018].

[16] "Atlac E-Nova MA 6215," [Online]. Available: https://aliancys.com/products/atlacr-e-nova-ma-6215/012074.pdf. [Accessed 31 05 2015].

[17] Aropol, "Technical Datasheet," [Online]. Available: http://www.kevytrakentajanverkkokauppa.fi/wp-content/uploads/Aropol-M105-TB-EG.pdf. [Accessed 26 05 2018].

[18] W. System, "Physical properties of West System epoxies," [Online]. Available: http://www.kevytrakentajanverkkokauppa.fi/wp-content/uploads/Aropol-M105-TB-EG.pdf. [Accessed 26 05 2018].

[19] J. C. W. C. W. Robert D. Adams, in *Structural Adhesive Joints in Engineering*, Chapman and Hall, 2-6 Boundary Row, London SE! 8HN UK, 1997.

[20] www.iso.org, "Standards Catalogues 83.180 - Adhesives," [Online]. Available: https://www.iso.org/ics/83.180/x/. [Accessed 25 05 2018].

[21] www.astm.org, "Adhesive Standards," [Online]. Available: https://www.astm.org/Standards/adhesive-standards.html. [Accessed 25 05 2018].

[22] www.astm.org, "Adhesive Standards," [Online]. Available: https://www.astm.org/Standards/adhesive-standards.html. [Accessed 25 05 2018].